RECOGNITION OF ONE CLASS OF QUADRIC SURFACES FROM UNSTRUCTURED POINT CLOUD

UDC: 004.896; 528.854;

Zivana Jakovljevic 1, Veljko Markovic 1

1 University of Belgrade, Faculty of Mechanical Engineering, Department for Production Engineering, Kraljice Marije 16, Belgrade, 11000, Serbia; zjakovljevic@mas.bg.ac.rs, markovicveljko@yahoo.com

Abstract: Critical elements of the state of the art three-dimensional (3D) point cloud processing software are the algorithms for retrieval of high level geometric primitives from raw data. This paper presents a method for recognition of a class of quadric surfaces, in particular for recognition of cylinders, elliptical cylinders, and ellipsoids from 3D point clouds. The method is based on direct least squares fitting of ellipsoids, and it exploits the closeness of scatter matrix to singular in the case when data are sampled for an approximate ellipsoid. This method belongs to the class of region growing methods, and the region is expanded using region growing strategy that is also proposed in this paper. Presented recognition procedure is suitable for segmentation of regions with G1 or higher continuality, and this is its advantage when compared to similar methods. Besides, recognition of quadric surfaces can be performed on unstructured, as well as on structured point clouds. The applicability of the method is illustrated and experimentally verified using two examples that contain G1 continuous surfaces from the considered class. The first example represents synthesized, and the second real-world scanned point cloud.

Key Words: 3D point cloud, surface recognition, quadrics segmentation, reverse engineering.

1. INTRODUCTION

Research efforts in the field of application of three – dimensional (3D) scanning devices in manufacturing are very intensive in the last few years [1]. Besides their traditional implementation in the reverse engineering, there have been research in implementation of 3D scanning devices in the various manufacturing processes such as quality control [2], robot grasping [3,4], robotic welding tasks [5,6], and mobile robots navigation [7].

Contemporary 3D scanning devices are characterized by high speed, resolution, and accuracy and provide point clouds with abundant data [8]. Generally, the application of 3D scanning devices has the following basic phases [9]: 1) data acquisition, 2) pre-processing, 3) surface recognition (segmentation and fitting), and 4) computer aided design (CAD) model creation. There exist a number of very efficient methods for point cloud pre-processing, i.e. for point cloud registration, integration, and meshing [9], and generation of aesthetically correct 3D model in the form of triangular mesh from point cloud is standard feature of the state of the art CAD systems. However, recognition of high level geometric primitives and generation of parametric 3D CAD model from point cloud is still an open research area.

Of all geometric primitives, the recognition of planar surfaces has attracted the most research efforts. There is a number of proposed methods for plane recognition that are based on application of 3D Hough transform [10], RANSAC (Random Sample Consensus) algorithm [11,12], various region growing methods [13,14], wavelet transform [15], etc.

In mechanical engineering, next to planar surfaces, the most important are rotational surfaces, in particular cylinders. Cylinders belong to the class of natural quadric surfaces. Recognition of quadrics has been in the focus of a number of research works. Proposed strategies for segmentation of quadrics from point cloud can be divided into two basic groups [16]: 1) strategies based on edge detection, and 2) strategies based on regions.

In edge based techniques, the edges (boundaries) between surfaces are first detected and the segmentation is carried out using obtained faces' boundaries. This approach is convenient for G0 continuous surfaces where there is an abrupt change between adjacent faces. However, for surfaces with G1 or higher continuity, it is very difficult to detect edges. It should be emphasized that in mechanical engineering a very large number of parts contains G1 continuous quadrics; this is usually a result of cutting tool radius.

Region based segmentation is carried out by split and merge approach or by region growing. In these methods, the points belonging to surfaces are clustered using different criteria. In the most of papers [17], [18,19] the algorithm for region growing starts from a chosen seed point and expands the region topologically to find the vertices which have similar geometric properties as seed point. Criteria for deciding which point will be attached to established cluster can be different. The most of them are based on features of differential geometry of surfaces such as local surface normal [18], average curvature [17], and principal curvatures [20]. In these methods the choice of seed point is as a rule carried out manually. Automatic choice of seed point can be a complex task. In [21] the authors for region growing method use automatically selected

seed region, not a single seed point; region growing algorithm is based on bicubic Bézier surface properties. RANSAC which randomly selects the region from the point cloud has been also employed for recognition of cylinders [12]. An approach for segmentation of quadrics from scanned lines that is based on numerically stable least squares fitting of ellipse is presented in [22]. However, this method is intended for segmentation of surfaces connected with G0 continuality.

In our previous research, we have proposed the method for recognition of elliptical segments in scanned lines [23], as well as the method for recognition of a class of natural quadrics from structured point clouds [24]. Proposed methods are based on direct least squares fitting of ellipse. Since, for some scanning devices the structured point clouds are not at disposal, in this paper we are extending the previous findings to the case of unstructured point cloud. In this research work we apply direct least squares fitting of ellipsoids to effectively recognize quadrics from unstructured point cloud. The proposed method is essentially region growing method that exploits the reciprocal condition number of scatter matrix for region growing. Unlike edge based methods, this method is convenient for effective segmentation of adjacent surfaces with G1 or higher continuality as will be illustrated using selected synthesized and scanned point clouds. The method can be applied for recognition of cylinders, elliptical cylinders and ellipsoids from point cloud.

The rest of the paper is organized as follows. In Section 2 we provide some theoretical background regarding direct least squares fitting of ellipsoids [25], [26]. Section 3 presents the method for recognition of considered class of quadrics which is implemented in Section 4 on a real-world example. Finally, in Section 5 we give concluding remarks.

2. DIRECT LEAST SQUARES FITTING OF ELLIPSOIDS

Quadric surface, in general, can be represented by the following equation:

$$a_1 x^2 + a_2 y^2 + a_3 z^2 + a_4 xy + a_5 yz + \\ a_6 xz + a_7 x + a_8 y + a_9 z + a_{10} = 0 \tag{1}$$

where a_i denote the surface parameters, and $[x, y, z]$ is the point on the surface. Equation (1) can be written in the matrix form:

$$\mathbf{x} \cdot \mathbf{a} = 0 \tag{2}$$

where $\mathbf{a} = [a_1\ a_2 \dots\ a_{10}]^T$ denotes the vector of surface parameters, and $\mathbf{x} = [x^2\ y^2\ z^2\ xy\ yz\ xz\ x\ y\ z\ 1]$.

Depending on the correlation between the values of coefficients a_i there are 17 different types of quadric surfaces [27]. In our case, the real ellipsoid and real elliptic cylinder are of interest. Namely, cylinder which is one of the most important surfaces in mechanical engineering represents a special class of real elliptic cylinder. On the other hand, real elliptic cylinder can be

observed as a degenerate real ellipsoid with the smaller ranks of specific matrices [27]. Having this in mind, the same fitting procedure can be applied for fitting all of these surfaces.

Starting from Fitzgibbon's direct least squares fitting of ellipse [25], in [26] a procedure for direct least squares fitting of ellipsoids was proposed. The procedure is based on the postulate that the section of ellipsoid and arbitrary plane represents an ellipse (the same holds for elliptic cylinder with the exception of parallel lines) and can be summarized as follows [26]. Coefficients $\mathbf{a}$ can be obtained by solving the minimization problem [26]:

$$min\|\mathbf{Da}\|^2 \\ subject\ to\ \mathbf{a}^T \mathbf{Ma} = 1 \tag{3}$$

In (3) matrix $\mathbf{D}$ is design matrix in the form:

$$\mathbf{D} = \begin{bmatrix} x_1^2 & x_2^2 & x_3^2 & \dots & x_N^2 \\ y_1^2 & y_2^2 & y_3^2 & \dots & y_N^2 \\ z_1^2 & z_2^2 & z_3^2 & \dots & z_N^2 \\ x_1 y_1 & x_2 y_2 & x_3 y_3 & \dots & x_N y_N \\ y_1 z_1 & y_2 z_2 & y_3 z_3 & \dots & y_N z_N \\ x_1 z_1 & x_2 z_2 & x_3 z_3 & \dots & x_N z_N \\ x_1 & x_2 & x_3 & \dots & x_N \\ y_1 & y_2 & y_3 & \dots & y_N \\ z_1 & z_2 & z_3 & \dots & z_N \\ 1 & 1 & 1 & \dots & 1 \end{bmatrix}^T \tag{4}$$

and matrix $\mathbf{M}$ has the dimension 10×10 with the following values [26]:

$\mathbf{M}(1, 2) = \mathbf{M}(2, 1) = 2,$ $\mathbf{M}(1, 3) = \mathbf{M}(3, 1) = 2\beta^2,$
$\mathbf{M}(2, 3) = \mathbf{M}(3, 2) = 2\alpha^2,$ $\mathbf{M}(1, 5) = \mathbf{M}(5, 1) = 2\beta,$
$\mathbf{M}(2, 6) = \mathbf{M}(6, 2) = 2\alpha,$ $\mathbf{M}(3, 4) = \mathbf{M}(4, 3) = -2\alpha\beta,$
$\mathbf{M}(4, 4) = -1,$ $\mathbf{M}(5, 4) = \mathbf{M}(4, 5) = -\alpha,$
$\mathbf{M}(5, 5) = -\alpha^2,$ $\mathbf{M}(6, 4) = \mathbf{M}(4, 6) = -\beta,$
$\mathbf{M}(6, 6) = -\beta^2,$ $\mathbf{M}(5, 6) = \mathbf{M}(6, 5) = \alpha\beta,$

and $\mathbf{M}(i, j) = 0$ otherwise. α and β are the parameters of arbitrary plane that intersects quadric surface:

$$z = \alpha x + \beta y + \gamma \tag{5}$$

Ellipsoidal solution of minimization problem (3) is single positive eigenvalue of [26]:

$$\mathbf{Sa} = \lambda \mathbf{Ma} \tag{6}$$

where

$$\mathbf{S} = \mathbf{D}^T \mathbf{D} \tag{7}$$

represents scatter matrix and λ is Lagrange multiplier.

As in the case of ellipse [25], when all points are sampled from an exact ellipsoid without noise, scatter matrix $\mathbf{S}$ will be close to singular.

3. METHOD FOR RECOGNITION OF POINTS BELONGING TO ONE CLASS OF QUADRIC SURFACES

The method that is proposed in this paper is intended for recognition (segmentation and fitting) of cylinders, real elliptical cylinders and real ellipsoids from point cloud. During recognition of regions belonging to different surfaces with G1 or higher continuality, when the surface is adequately segmented from point cloud, the problem of estimation of its parameters is relatively easily solved. In our method, segmentation is based on singularity of scatter matrix **S** (7) in the case when all the points are sampled from an exact ellipsoid.
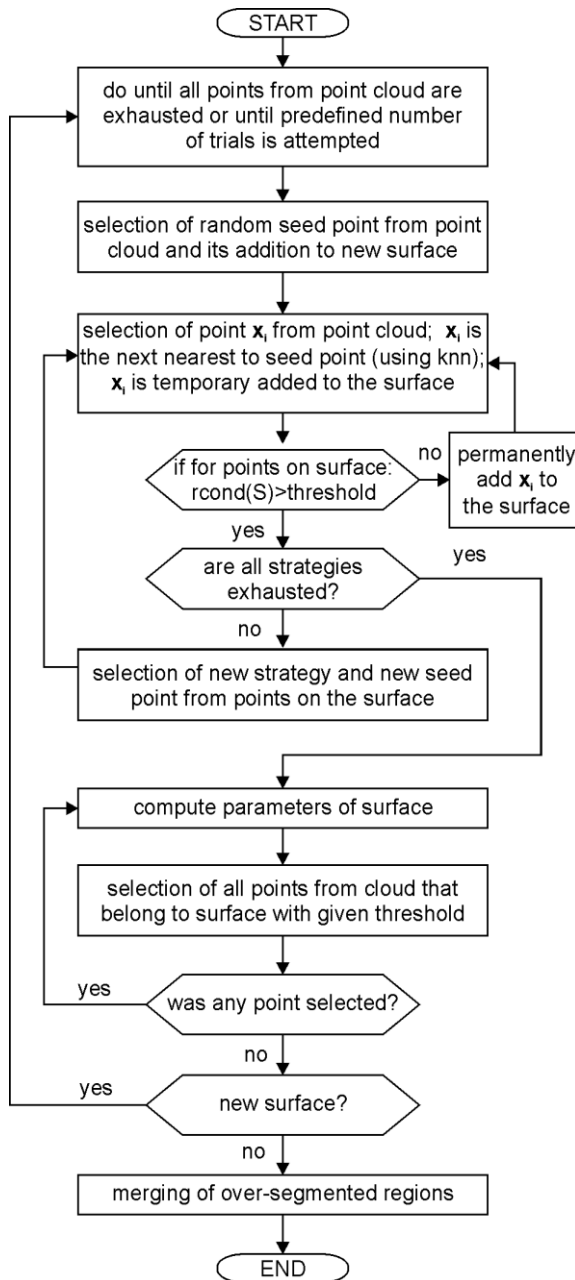

Figure 1. Algorithm of the method for recognition of a class of quadrics from point cloud

When points are sampled from an approximate ellipsoid, e.g. scanned points, than scatter matrix will not be singular, but it will be close to singular and its reciprocal condition number will be close to zero. If the points do not belong to an approximate ellipsoid, the reciprocal condition number will be higher. This property of reciprocal condition number can be exploited for generation of the algorithm for segmentation (and fitting) of ellipsoidal segments from point cloud.

The overview of our method can be presented by algorithm from Figure 1. The method starts with random selection of seed point. The region is grown around this point by subsequent selection of the points from cloud using the strategy that will be presented in the sequel. During region expanding new point is temporarily added to the region, and the reciprocal condition number of scatter matrix **S** (7) for points in the region is computed. If the value of reciprocal condition number is smaller than the predefined threshold, the point is permanently added to the region. The procedure is repeated until there are no more points in the point cloud that can be added to the region using proposed region growing strategy. When region is created, the algorithm computes the parameters of the surface represented by points from the region and extracts all the points from point cloud that belong to given surface with predefined threshold using procedure that will be explained in one of the following subsections. In such a way algorithm segments one region from point cloud that contains points belonging to one surface from the considered class of quadrics.

The presented segmentation procedure is repeated until all the points from the cloud are exhausted in the case when the point cloud contains only the considered class of quadric surfaces. In the case when there are other surfaces in the point cloud, the procedure stops when the number of unsuccessful trials crosses over predefined value.

The presented algorithm can lead to over-segmentation of certain regions. In order to overcome this issue, the segments that belong to the same surfaces are merged based on estimated surface parameters.

3.1 Region growing strategy

The region growing starts by determining the nearest-neighbors of seed point using K-nearest-neighbors (kNN) algorithm. kNN is well-known nonparametric method which is used in pattern recognition for classification and regression [28], [29], [30]. In 3D space kNN selects the data (in our case points) with smallest algebraic distance from one chosen sample. Distance can be calculated by using many different distance functions (e.g., Euclidean, Manhattan, Lagrange...) [28].

In this paper we employ kNN for finding and sorting the points from point cloud according to their distance from seed point. Distances between seed point $[x_s, y_s, z_s]$ and other points from the cloud $[x_i, y_i, z_i]$, $i=1$, N-1,

355

where N denotes the number of points in the cloud, are determined using Euclidian distance:

$$d = \sqrt{(x_s - x_i)^2 + (y_s - y_i)^2 + (z_s - z_i)^2} \quad (8)$$

During region growing, points are in succeeding order added to the region according to their vicinity to the seed point, if the value of reciprocal condition number of matrix **S** is below predefined threshold. Since we utilize Euclidian distance, the points that are added to the region are within a sphere whose centre is in the seed point – Figure 2a.
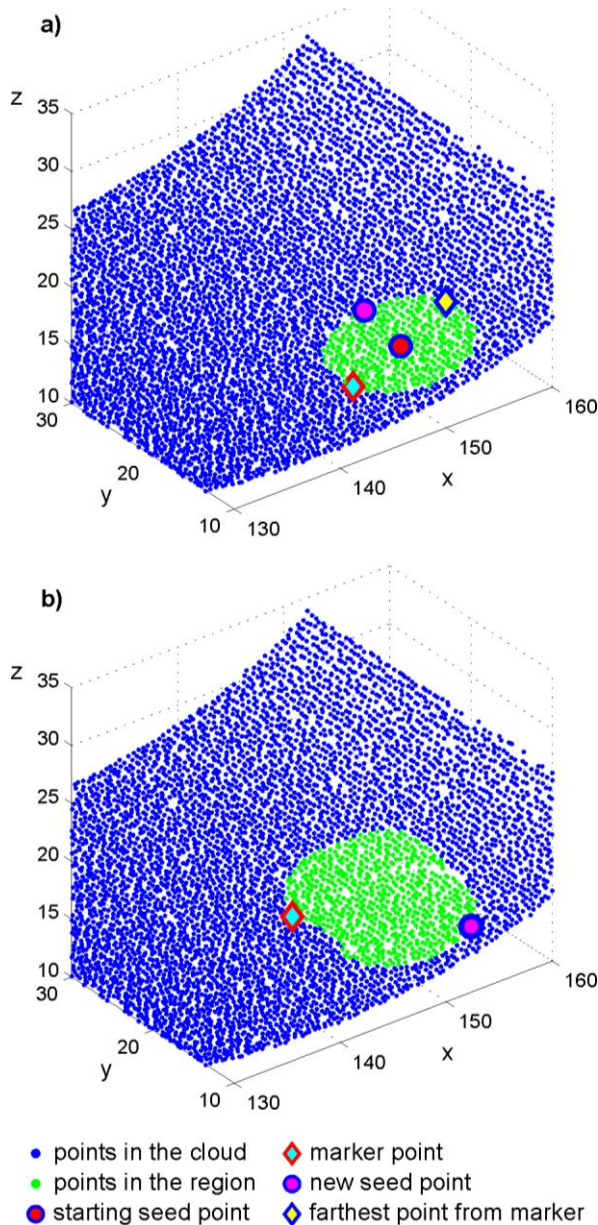

Figure 2. Region growing and new seed selection: a) strategy 1; b) strategy 2

When we find a marker point $[x_m, y_m, z_m]$ – point from the cloud that does not belong to the surface, i.e. the point for which reciprocal condition number of **S** crosses over predefined threshold, new seed point should be selected in order to further expand the region

if possible. For selection of new seed point we sequentially employ one of the three strategies until all strategies are employed and no more points can be added to the region. The strategies are as follows.

Strategy 1: New seed point is the point which is "half way" between the marker point and the point with the largest distance from the marker when points added to the cloud using current seed are considered. Let marker be n^{th} point in the region and the point with largest distance m^{th} point in the region. The index of new seed point will be rounded value of (m+n)/2. Since the points in the cloud are stochastically distributed, and region is expanded spirally, it is expected that the position of new seed point will be near the half of the arc between marker and the point with largest distance from it. An example of the application of strategy 1 is presented in Figure 2a.

Strategy 2: New seed point is the point from the region that has the largest distance from marker. An example of application of strategy 2 is presented in Figure 2b.

Strategy 3: New seed point is in the vicinity of the marker – this is the point that was added to the region five cycles before adding marker.

3.2 Segmentation of surfaces using generated regions and merging over-segmented regions

When algorithm finds the region using previously defined strategy, it can proceed with segmentation of one surface from point cloud. For the points in the region, the parameters of equation (1) are computed. Ellipsoid surface parameters represent the eigenvector that corresponds to the single positive eigenvalue of (6) [26]. The parameters α and β of arbitrary plane for matrix **M** are computed utilizing the first two points added to the region – $[x_1, y_1, z_1]$ and $[x_2, y_2, z_2]$ and one of the following equations:

$$\mathbf{n} = \begin{bmatrix} x_1 - x_2 & y_1 - y_2 & z_1 - z_2 \end{bmatrix} \times \begin{bmatrix} 1 & 1 & 1 \end{bmatrix} \quad (9)$$

$$\mathbf{n} = \begin{bmatrix} x_1 - x_2 & y_1 - y_2 & z_1 - z_2 \end{bmatrix} \times \begin{bmatrix} 1 & 1 & 0.5 \end{bmatrix} \quad (10)$$

In (9) and (10) **n** is the normal vector of arbitrary plane, and $\alpha = -\mathbf{n}(1)/\mathbf{n}(3)$, $\beta = -\mathbf{n}(2)/\mathbf{n}(3)$.

When the parameters of the surface are known, algorithm can extract all the points from the point cloud that belong to this surface with predefined threshold. For extracted points new ellipsoid surface parameters can be computed and the procedure can be cyclically repeated until no more points from the cloud can be added to the surface.

In some situations the algorithm can lead to over-segmentation as will be illustrated in one of the examples in the sequel. For these cases, the procedure for merging will find the regions that belong to the same surface. In merging procedure, two regions are temporarily merged and parameters of ellipsoid surface are estimated. If the points from both regions belong to the estimated surface with predefined threshold the

regions are permanently merged. Otherwise they remain separated.

3.3 Verification of the presented method using synthesized point cloud

The applicability of the presented method is illustrated using a synthesized unstructured point cloud. The point cloud is made of three real elliptic cylinders with G1 continuality – Figure 3a. Parameters of the used real elliptic cylinders are presented in Table 1. To the synthesized point cloud a noise of 90 dB was added. From the synthesized point cloud with noise, the proposed methodology segmented the regions as illustrated in Figure 3b. As can be observed from the Figure 3, the method has adequately segmented the regions that correspond to elliptical cylinders.

The parameters of synthesized surfaces for segments 1-3 from Figure 3 along with estimated surface parameters using presented methodology are presented in Table 1. An excellent agreement between estimated and input parameters can be observed. Maximum relative error between corresponding coefficients is for coefficient a_7 of the first segment and it equals 5.41%. Notice that in the most cases the method has adequately estimated that the value of coefficients equals zero.

The employed threshold for reciprocal condition number was 0.5×10^{-19}, and the threshold for detection of points from point cloud that belong to recognized surface was 5×10^{-5}.
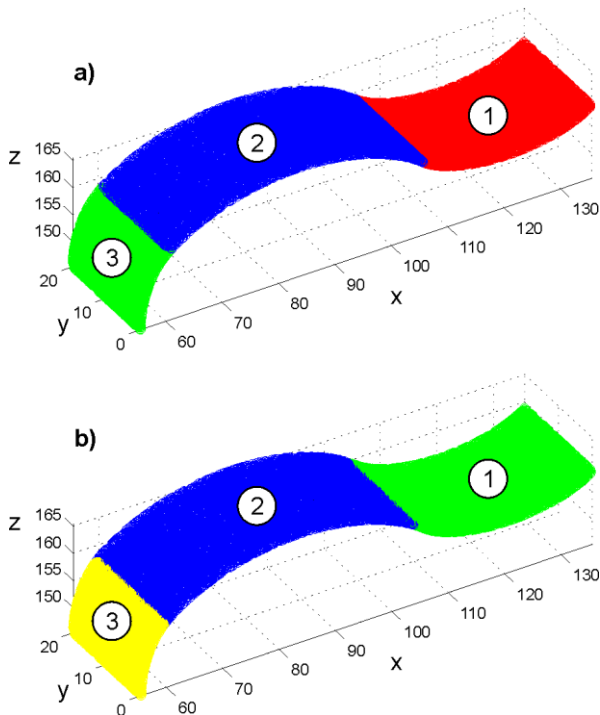

Figure 3. Synthesized signal: a) Original segments; b) Recognized segments using proposed method

For surface denoted by 2 in Figure 3, the initial region obtained after application of proposed region growing strategy is presented in Figure 4a. After initial region

determination segmentation procedure was performed as follows. In each step/cycle of segmentation procedure, new parameters of the surface are computed and points that belong to this surface with predefined threshold are added to the region. For surface denoted by 2 in Figure 3 the procedure contained three cycles, and after the third cycle no more points could be added to the surface. In the first cycle 1217 points were added to the region, in the second 1013 points, while in the third cycle the region was expanded by 675 points. The points added to the region in each cycle are presented in Figure 4b.

○ points in the region obtained using proposed region growing strategy

○ points added to the region in the first cycle of segmentation

○ points added to the region in the second cycle of segmentation

○ points added to the region in the third cycle of segmentation
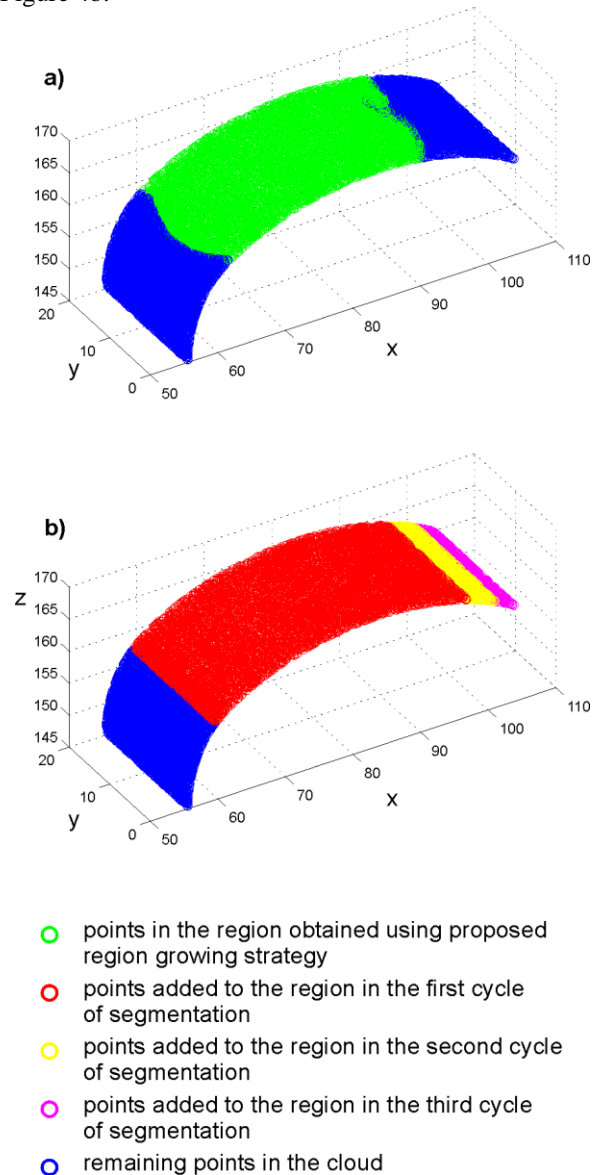
○ remaining points in the cloud

Figure 4. Segmentation of surface 2 from Figure 3: a) initial region obtained using region growing strategy; b) points added to the region using segmentation procedure

Table 1. Synthesized and estimated parameters of surfaces from Figure 3

		Surface equation: $a_1x^2 + a_2y^2 + a_3z^2 + a_4xy + a_5yz + a_6xz + a_7x + a_8y + a_9z + 1 = 0$ coefficients $[a_i \times 10^3]$, i=1,…9								
Synthesized surface parameters (Figure 3a)	Segment 1	[0.0072	0	0.0338	0	0	0	-1.7451	0	-11.007]
	Segment 2	[0.0195	-0.0016	0.0427	0	0	0	-3.0050	0	-12.275]
	Segment 3	[0.0704	0	0.0333	0	0	0	-9.2313	0	-9.6921]
Estimated surface parameters (Figure 3b)	Segment 1	[0.0076	0.0000	0.0333	-0.0000	0.0001	0.0002	-1.8538	-0.0103	-10.901]
	Segment 2	[0.0190	0.0000	0.0425	-0.0000	0.0000	-0.0015	-2.9273	-0.0030	-12.274]
	Segment 3	[0.0704	0.0000	0.0333	0.0000	-0.0000	0.0000	-9.2304	0.0000	-9.6913]

4. EXPERIMENTAL VERIFICATION OF THE PRESENTED METHOD

The presented method is experimentally verified using a real-world part presented in Figure 5. This part represents a typical benchmark test utilized in many studies referring to the recognition of geometric primitives from point cloud [15,16,31]. The part was scanned using ATOS Compact Scan 3D scanning device by GOM mbh, and unstructured point cloud was obtained. In this study we have analyzed the surface marked red on the CAD model presented in Figure 6. The surface consists of 5 cylindrical segments with G1 continuality. Before proceeding with the analysis of obtained results, it is important to emphasize that the part was made on three-axis machining center and that it is characterized by extremely poor quality as can be observed from Figure 5.

The results of segmentation using proposed procedure are presented in Figure 7. The applied threshold for reciprocal condition number of matrix **S** was 10^{-20}, while the threshold for segmentation using estimated parameters was 0.000053.

Initially the algorithm over-segmented surfaces and found seven segments as presented in Figure 7a. However, after application of the algorithm for merging the regions which can be approximated with one surface as explained in subsection 3.2, we have obtained adequate segmentation that is presented in Figure 7b.
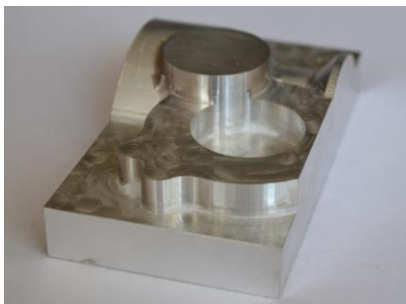

Figure 5. A photograph of a real-world part used for experimental verification of the proposed method

Table 2 presents the estimated parameters of segmented surfaces from Figure 7b. Estimation was performed using direct least fitting squares of ellipsoids from Section 2.

From Table 2, it can be observed that coefficients a_1, for all five segments are close to zero when compared to coefficients a_2 and a_3. This shows that the main axes of the surfaces are almost parallel to x axis. Besides, for segments 3 and 5 coefficients a_7 are close to zero when compared to a_8 and a_9.
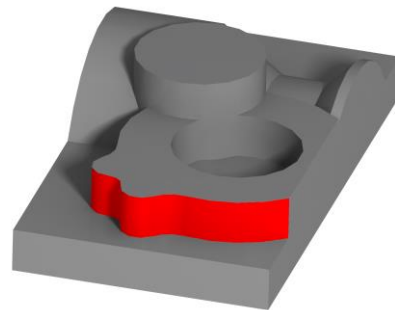

Figure 6. CAD model of a test part – the surface of interest is marked red

If from estimated parameters only the first four digits after decimal point are taken as significant, than the ranks of matrices **e** and **E**:

$$\mathbf{e} = \begin{bmatrix} a_1 & \dfrac{a_4}{2} & \dfrac{a_6}{2} \\ \dfrac{a_4}{2} & a_2 & \dfrac{a_5}{2} \\ \dfrac{a_6}{2} & \dfrac{a_5}{2} & a_3 \end{bmatrix} \quad \mathbf{E} = \begin{bmatrix} a_1 & \dfrac{a_4}{2} & \dfrac{a_6}{2} & \dfrac{a_7}{2} \\ \dfrac{a_4}{2} & a_2 & \dfrac{a_5}{2} & \dfrac{a_8}{2} \\ \dfrac{a_6}{2} & \dfrac{a_5}{2} & a_3 & \dfrac{a_9}{2} \\ \dfrac{a_7}{2} & \dfrac{a_8}{2} & \dfrac{a_9}{2} & 1 \end{bmatrix} \quad (11)$$

are equal to 2 and 4 for regions 1, 2 and 4, i.e., 2 and 3 for regions 3 and 5 from Figure 7b. The determinant of matrix **E** is less than zero for regions 1, 2 and 4. In addition, the nonzero eigen values of matrix **e** have the same sign, while the nonzero eigen values of matrix **E** have the opposite signs. These findings show that regions 1, 2 and 4 represent elliptic paraboloids and regions 3 and 5 real elliptic cylinders [27].

Table 2. Estimated parameters of surfaces from Figure 7b

| Surface equation: $a_1x^2 + a_2y^2 + a_3z^2 + a_4xy + a_5yz + a_6xz + a_7x + a_8y + a_9z + 1 = 0$ coefficients $[a_i \times 10^3]$, i=1,…9									
Segment 1	[0.0014	0.0703	0.1910	0.0041	-0.0808	-0.0144	1.0984	4.5499	-27.6839]
Segment 2	[0.0029	0.1292	0.1184	0.0037	0.0177	-0.0107	0.7093	-6.6538	-21.2488]
Segment 3	[-0.0005	0.1455	0.1365	-0.0002	-0.0058	0.0002	0.0016	-7.5242	-22.0723]
Segment 4	[0.0012	0.1611	0.1477	0.0009	-0.0792	0.0009	-0.1454	-4.9455	-21.8520]
Segment 5	[-0.0006	0.1461	0.1418	0.0008	0.0074	0.0007	-0.0578	-10.8495	-21.5807]
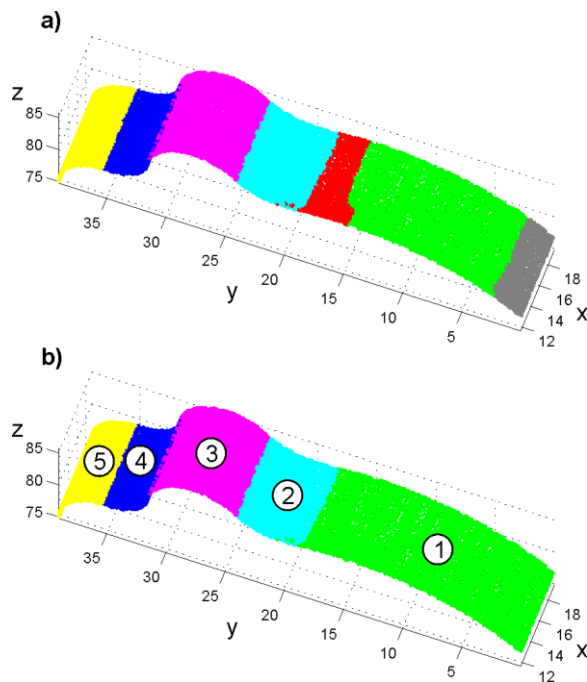
Figure 7. Segmentation of the scanned part from Figure 5: a) initial segmentation; b) segmentation after merging of over-segmented regions

5. CONCLUSION

In this paper we have presented our research in the field of recognition (segmentation and fitting) of a class of quadrics from 3D point cloud. The objective of our research was to extract cylindrical regions from point cloud. However, since the presented procedure is based on direct least squares fitting of ellipsoids, it can be applied for segmentation of all quadric surfaces whose cross section with plane is in the form of ellipse. The method belongs to the class of region growing methods and it uses the closeness of scatter matrix to singular as basic region growing criterion. Region growing is carried out using kNN algorithm in combination with several strategies for further region expanding. Very important property of the method is that it is suitable for segmentation of G1 (or higher) continuous surfaces from unstructured point cloud.

We have illustrated the performances of the presented method using two case studies. In the first case study which considers the synthesized point cloud with noise, the method was able to adequately segment cylindrical regions. The values of estimated surface parameters had adequate relative errors to the parameters of synthesized surfaces. In the second, real world, case study, the method has also adequately segmented surfaces. Two of the recognized surfaces belong to the class of cylinders, while three of them belong to the class of elliptic paraboloids. The part was designed in such a way that all of the considered surfaces were cylinders. However, since the quality of the machined part was very low (it was made on three-axis machining centre), the recognition procedure has shown good results.

As a part of following research efforts we plan to join this method to previously introduced wavelet based method for recognition of planar segments [15]. Besides, the analysis of sensitivity of the presented method to the selection of seed point will be in the focus of future research.

ACKNOWLEDGEMENT

REFERENCE

[1] Bi, Z.M., Wang, L., *Advances in 3D data acquisition and processing for industrial applications*, Robotics and Computer-Integrated Manufacturing, Vol.26, No.5, pp.403-413, 2010.

[2] Xu, J., Xi, N., Zhang, C., Shi, Q., Gregory, J., *A Robot-Assisted Back-Imaging Measurement System for Transparent Glass*, IEEE/ASME Transactions on Mechatronics, Vol.17, No. 4, pp.779 – 788, 2012.

[3] Kim, J., Nguyen, H.H., Lee, Y., Lee, S., *Structured light camera base 3D visual perception and tracking application system with robot grasping task*, IEEE International Symposium on Assembly and Manufacturing (ISAM), pp.187 – 192, 2013.

[4] Effenberger, I., Kühnle, J., Verl, A., *Fast and flexible 3D object recognition solutions for machine vision applications*, Proc. of SPIE-IS&T Electronic Imaging, Image Processing: Machine Vision Applications VI, Vol.8661, pp.86610N-1-86610N-10, 2013.

[5] Rodrigues, M., Kormann, M., Schuhler, C., Tomek, P., *Structured Light Techniques for 3D Surface Reconstruction*

in Robotic Tasks, Proceedings of the 8th International Conference on Computer Recognition Systems CORES, Advances in Intelligent Systems and Computing, Vol.226, pp.805-814, 2013.

[6] Fang, Z., Xu, D., Tan, M., *A Vision-Based Self-Tuning Fuzzy Controller for Fillet Weld Seam Tracking*, IEEE/ASME Transactions on Mechatronics, Vol.16, No.3, pp.540 – 550, 2011.

[7] Fu, G., Corradi, P., Menciassi, A., Dario, P., *An Integrated Triangulation Laser Scanner for Obstacle Detection of Miniature Mobile Robots in Indoor Environment*, IEEE/ASME Transactions on Mechatronics, Vol.16, No.4, pp.778 – 783, 2011.

[8] Savio, E., De Chiffre, L., Schmitt, R., *Metrology of freeform shaped parts*, Annals of the CIRP, Vol.56, No.2, pp.810-834, 2007.

[9] Varady, T., Martin, R.R., Cox, J., Reverse engineering of geometric models – an introduction, Computer Aided Design, 29, p.p. 255-268, 1997.

[10] Borrmann, D., Elseberg, J., Lingemann, K., Nuechter, A., *The 3D Hough transform for plane detection in point clouds: a review and a new accumulator design*, *3DR Expresss*, Vol.2, No.2, Art.No.3, pp.1-13, 2011.

[11] Fischler, M.A., Bolles, R.C., *Random Sample Consensus: A paradigm for model fitting with application to image analysis and automated cartography*, Communications of ACM, Vol.24, pp.381-395, 1981.

[12] Schnabel, R., Wahl, R., Klein, R., *Efficient RANSAC for Point-Cloud Shape Detection*, Computer Graphics Forum, Vol.26, No.2, pp.214–226, 2007.

[13] Nguyen, H.H., Kim, J., Lee, Y., Ahmed, N., Lee, S., *Accurate and fast extraction of planar surface patches from 3D point cloud*, Proceedings of 7th International Conference on Ubiquitous Information Management and Communication, pp. 84:1-84:8, 2013.

[14] Wang, L., Cao, J, Han, C., *Multidimensional particle swarm optimization-based unsupervised planar segmentation algorithm of unorganized point clouds*, Pattern Recognition, Vol.45, No.11, pp4034–4043, 2012.

[15] Jakovljevic, Z., Puzovic, R., Pajic, M., *Recognition of Planar Segments in Point Cloud based on Wavelet Transform*, IEEE Transactions on Industrial Informatics, 2015, doi: 10.1109/TII.2015.2389195

[16] Petitjean, S., *A Survey of Methods for Recovering Quadrics in Triangle Meshes*, ACM Computing Surveys, Vol.2, No.34, pp.1-61, 2002.

[17] Lai, H.C., Chang, Y.H., Lai, J.Y., *Development of feature segmentation algorithms for quadratic surfaces*, Advances in Engineering Software, Vol.40, No.10, pp.1011–1022, 2009.

[18] Rabbani, T., Van den Heuvel, F.A., Vosselman, G., *Segmentation of point clouds using smoothness constraint,*

International Archives of Photogrammetry, Remote Sensing and Spatial Information Sciences, Vol.36, No.5, pp.248-253, 2006.

[19] Vančo, M., Hamann B., Brunnett, G., *Surface Reconstruction from Unorganized Point Data with Quadrics,* Computer Graphics Forum, Vol.27, No.6, pp.1593–1606, 2008.

[20] Lavoue, G., Dupont F., Baskurt A., *Curvature Tensor Based Triangle Mesh Segmentation with Boundary Rectification*, Proceedings of the Computer Graphics International, pp. 10-17, IEEE, 2004.

[21] Vieira, M., Shimada, K., *Surface mesh segmentation and smooth surface extraction through region growing*, Computer Aided Geometric Design, Vol. 22, No.8, pp.771-792, 2005.

[22] Rahayem, M.R., Kjellander, J.A.P., *Quadric segmentation and fitting of data captured by a laser profile scanner mounted on an industrial robot*, International Journal of Advanced Manufacturing Technology, Vol.52, No.1-4, pp.155–169, 2011

[23] Jakovljevic, Z., Markovic, V., Miladinovic, M., *Recognition of elliptical segments in scanned lines*, Etikum, pp.19-22, FTN, Novi Sad, 2014.

[24] Markovic, V., Jakovljevic, Z, *Segmentation of one class of quadric surfaces from structured point clouds*, 39th JUPITER Conference, Belgrade, pp.4-13-4.22, 2014. (in Serbian)

[25] Fitzgibbon, A., Pilu, M., Fisher R.B., *Direct Least Square Fitting of Ellipses*, IEEE Transactions on Pattern Analysis, Vol.21, No.5, pp.476-480, 1999.

[26] Ying, X., Yang, L., Kong, J., Hou, Y., Guan, S., Zha, H., *Direct least square fitting of ellipsoids*, Proceedings of the 21st International Conference on Pattern Recognition (ICPR), IEEE, pp.3228-3231, 2012.

[27] Zwillinger, D., *CRC Standard Mathematical Tables and Formulae - 31st Edition*, CRC Press, 2003.

[28] Webb, A., Copsey, K., *Statistical Pattern Recognition - Third Edition,* John Wiley & Sons, UK, 2011.

[29] Fukunaga, K., *Introduction to Statistical Pattern Recognition - Second Edition,* Academic Press, San Diego, USA, 1990.

[30] Zhang, M.L., Zhou, Z.H., *A k-nearest neighbor based algorithm for multi-label classification,* IEEE International Conference on Granular Computing, IEEE, Vol.2, pp.718-721, 2005.

[31] Kjellander, J.A.P., Rahayem, M., *Planar segmentation of data from a laser profile scanner mounted on an industrial robot*, International Journal of Advanced Manufacturing Technology, Vol.45, No1-2, pp.181-190, 2009.